Available online at www.sciencedirect.com

ScienceDirect

Procedia Computer Science 00 (2022) 1–19

Procedia Computer Science

Abstract

The Hybrid High Order (HHO) method is a powerful discretization method which has only been recently applied from to non linear computational mechanics.

The Hybrid High Order method divides the domain of interest in cells of arbitrary polyhedral shape, whose boundaries is called the skeleton, and introduces two kinds of degrees of freedom: the displacements in the cell and the displacements of the skeleton.

Most introductory materials to the HHO method is focus on the mathematical aspects of the methods. While those aspects are important, an approach based on physical considerations would help spreading this method to the computational mechanics and engineering communities.

This paper derives Hybrid High Order method from the classical Hu–Washizu functional.

Practical implementation of the method is discussed in depth using notations closed to the ones used in standard finite elements textbooks, highlighting the use of polyhedral cells and the use of approximation spaces based on polynomials of arbitrary orders.

From the point of view of numerical performances, the elimination of the cell degrees of freedom is mandatory to to reduce the size of the stiffness matrix. The standard static condensation, is presented, as well as a novel strategy called "cell equilibrium". Advantages and disadvantages of both strategies are discussed.

The resolution of axi-symmetrical problems, which has seldom, if ever, been discussed in the literature, is then presented.

Numerical examples prove the robustness of the method with regards to volumetric locking....

Keywords:
Computational mechanics, Hybrid High Order method, Static condensation, Cell equilibrium algorithm, Volumetric locking, Axi-symmetric modelling hypothesis

1. Introduction

The origin of DG methods dates back to the pioneering work of [1], where an hyperbolic formualtion is used to solve the neutron transport equation.

2. The model problem

Paragraph **??** introduces the classical Hu–Washizu functional to describe the quasi-static equilibrium of a body submitted to external load and the main notations used in this paper. For the sake of simplicity, the body is assumed hyper-elastic in this section.

Paragraph **??** introduces the classical Hu–Washizu functional to describe the quasi-static equilibrium of a body submitted to external load and the main notations used in this paper. For the sake of simplicity, the body is assumed hyper-elastic in this section.

Paragraph **??** introduces the key idea of the HHO method, which is to divide the domain in arbitrary subdomains connected by cohesive interfaces and to apply the Hu–Washizu functional to each sub-domains.

2.1. The standard Hu–Washizu lagragian

This paragraph introduces the standard Hu–Washizu three field principle. For the sake of simplicity, and without loss of generality, we consider the case of an hyperelastic material. Extensions to mechanical behaviours with internal state variables is treated in classical textbooks of computational mechanics. We will treat this extension in the Section 6 discussing the numerical implementation of the Hybrid High Order method and in Section 7 which provides several examples in plasticity.

2.1.1. Description of the mechanical problem and notations

Let us consider a solid body whose reference configuration is denoted Ω. At a given time $t > 0$, the body is in the current configuration Ω_t.

Mechanical loading. The body is assumed to be submitted to a body force $\boldsymbol{f}_v$ acting in Ω_t, a prescribed displacement $\boldsymbol{u}_d$ on the Dirichlet boundary $\partial_d\Omega_t$, a contact load $\boldsymbol{t}_n$ on the Neumann boundary $\partial_n\Omega_t$.

Deformation. $\boldsymbol{\Phi}$ denotes the deformation mapping the reference configuration $\partial\Omega$ to the current configuration$\partial\Omega_t$:

$$\boldsymbol{\Phi}(\boldsymbol{X}) = \boldsymbol{x} = \boldsymbol{X} + \boldsymbol{u}(X)$$

where $\boldsymbol{X}$, $\boldsymbol{x}$ and $\boldsymbol{u}$ denote respectively the position in the reference configuration $\partial\Omega$, the position in the current configuration $\partial\Omega$ and the displacement.

Deformation gradient, gradient of the displacement. The deformation gradient $\underset{\sim}{\boldsymbol{F}}$ is defined as:

$$\underset{\sim}{\boldsymbol{F}} = \nabla_{\boldsymbol{X}}\boldsymbol{\Phi} = \underset{\sim}{\boldsymbol{I}} + \nabla_{\boldsymbol{X}}\boldsymbol{u} = \underset{\sim}{\boldsymbol{I}} + \underset{\sim}{\boldsymbol{G}}$$

where $\nabla_{\boldsymbol{X}}$ is the gradient operator in the reference configuration and $\underset{\sim}{\boldsymbol{G}}$ denotes the gradient of the displacement.

Hyperelastic material. The body is assumed made of an hyperelastic material described by a free energy ψ which relates the deformation gradient $\underset{\sim}{\boldsymbol{F}}$ and the first Piola-Kirchhoff stress as follows:

$$\underset{\sim}{\boldsymbol{P}} = \frac{\partial\psi}{\partial\underset{\sim}{\boldsymbol{F}}}$$

Total lagrangian. The total Lagrangian L of the body is defined as the stored energy minus the work of external loadings as follows:

$$L(u) = \int_\Omega \psi\left(\underset{\sim}{\boldsymbol{F}}(\boldsymbol{u})\right) - \int_\Omega \boldsymbol{f}_V \cdot \delta\boldsymbol{u} - \int_{\partial_N\Omega} \boldsymbol{t}_N \cdot \delta\boldsymbol{u}|_{\partial_N\Omega} \tag{1}$$

where the body forces $\boldsymbol{f}_V$ and conctat tractions $\boldsymbol{t}_N$ in the reference configuration have been obtained from their counterparts $\boldsymbol{f}_v$ and $\boldsymbol{t}_n$ thanks to the Nanson formulae, i.e. $\boldsymbol{f}_V = ...$ and $\boldsymbol{f}_V = ...$

Variational characterisation of the mechanical equilibrium. The displacement $\boldsymbol{u}$ satisfying the mechanical equilibrium minimises the Lagragian L:

$$\boldsymbol{u} = \underset{\boldsymbol{u}^\star \in U(\Omega)}{\operatorname{argmin}} \; L\left(\boldsymbol{u}^\star\right)$$

where $U(\Omega)$ denotes the set of admissible displacements. Taking the first order variation of Lagrangian yields the principle of virtual work:

$$\int_\Omega \underset{\sim}{\boldsymbol{P}} : \nabla\delta\boldsymbol{u} = \int_\Omega \boldsymbol{f}_V \cdot \delta\boldsymbol{u} + \int_{\partial_N\Omega} \boldsymbol{t}_N \cdot \delta\boldsymbol{u}$$

2.2. Hu-Washizu Lagrangian

Hu-Washizu generalises the previous variational principle by considering that the gradient of the displacement $\underset{\sim}{\boldsymbol{G}}$ and the first Piola-Kirchoff $\underset{\sim}{\boldsymbol{P}}$ stress are independant unknowns of the problem.

The Hu-Washizu Lagrangian L^{HW} is then defined as follows:

$$L^{HW}\left(\boldsymbol{u}, \underset{\sim}{\boldsymbol{G}}, \underset{\sim}{\boldsymbol{P}}\right) = \int_\Omega \psi\left(\underset{\sim}{\boldsymbol{I}} + \underset{\sim}{\boldsymbol{G}}\right) + (\nabla \boldsymbol{u} - \underset{\sim}{\boldsymbol{G}}) : \underset{\sim}{\boldsymbol{P}} - \int_\Omega \boldsymbol{f}_V \cdot \boldsymbol{u} - \int_{\partial_N \Omega} \boldsymbol{t}_N \cdot \boldsymbol{u}$$

and the solution $\boldsymbol{u}$, $\underset{\sim}{\boldsymbol{G}}$ and $\underset{\sim}{\boldsymbol{P}}$ minimize the Hu-Washizu Lagrangian L^{HW}:

$$\left(\boldsymbol{u},\ \underset{\sim}{\boldsymbol{G}},\ \underset{\sim}{\boldsymbol{P}}\right) = \underset{\substack{\boldsymbol{u}^\star \in U(\Omega), \\ \underset{\sim}{\boldsymbol{G}}^\star, \underset{\sim}{\boldsymbol{P}}^\star}}{\operatorname{argmin}} L\left(\boldsymbol{u}^\star, \underset{\sim}{\boldsymbol{G}}^\star, \underset{\sim}{\boldsymbol{P}}^\star\right)$$

The first order variation of the Hu-Washizu Lagragian with respect to $\boldsymbol{u}$, $\underset{\sim}{\boldsymbol{G}}$, $\underset{\sim}{\boldsymbol{P}}$ yields:

$$\frac{\delta L^{HW}}{\delta \boldsymbol{u}} = \int_\Omega \underset{\sim}{\boldsymbol{P}} \cdot \nabla \delta \boldsymbol{u} - \int_\Omega \boldsymbol{f}_V \cdot \delta \boldsymbol{u} - \int_{\partial_N \Omega} \boldsymbol{t}_N \cdot \delta \boldsymbol{u} \tag{2a}$$

$$\frac{\delta L^{HW}}{\delta \underset{\sim}{\boldsymbol{P}}} = \int_\Omega \left(\nabla \boldsymbol{u} - \underset{\sim}{\boldsymbol{G}}\right) \cdot \delta \underset{\sim}{\boldsymbol{P}} \tag{2b}$$

$$\frac{\delta L^{HW}}{\delta \underset{\sim}{\boldsymbol{G}}} = \int_\Omega \left(\frac{\partial \psi}{\partial \underset{\sim}{\boldsymbol{G}}} - \underset{\sim}{\boldsymbol{P}}\right) \cdot \delta \underset{\sim}{\boldsymbol{G}} \tag{2c}$$

Equation (2b) shows that $\underset{\sim}{\boldsymbol{G}}$ is equal to $\nabla \boldsymbol{u}$ is a weak sense and Equation (2c) shows that the First Piola Kirchhoff stress is equal to the derivative the free energy in a weak sense.

Some words about the importance of the Hu-Washizu principle.

3. Introduction to discontinuous methods through a Hu-Washizu formulation

Many numerical methods, including the finite element method, considers a partition of the body into elementary subsets. Let T be such a subset and let ∂T be its boundary. For the sake of simplicity, the intersection of ∂T and $\partial \Omega$ is first assumed empty. This special case is treated later.

3.1. Mechanical equilibrium between T and $\Omega \backslash T$

...

Dans le problème présenté Section 2, les champs d'inconnues sont définis sur l'ensemble de la structure Ω. Toutefois, les méthodes (hybrides) discontinues supposent la discontinuité du champ d'inconnues au sein même du solide. Afin d'intruduire naturellement le problème variationnel propores aux méthodes discontinues à partir du cadre continu tel que décrit Section 2, on considère un matériau composite, constitué d'une matrice dont le volume est négligeable devant celui du renfort.

3.2. Interest zone description

Dans ce contexte, let $T \subset \Omega$ an arbitrary subset of the solid body, with boundary ∂T that is subjected to a contact load $\boldsymbol{t}_{\partial_N T}$. Dans un soucis de simplification, on suppose T polyédrique, convex et à faces planes. Le volume T réprésente une portion de ce matériau composite, que l'on décompose en une partie de renfort, notée $K \subset T$ with boundary ∂K, et en une partie périphérique $I \subset T$ représentant la matrice et entourant le renfort K. On note $\partial I = \partial K \cup \partial T$ la frontière de la matrice. La matrice se présente sous forme d'une bande d'épaisseur $\ell > 0$ that is supposed to be small compared to h_T the diameter of T (see Figure 1), de sorte qu'on introduit l'homotethy $\boldsymbol{\Xi}_T$ of ratio $(1 - \alpha\ell)$ and center $\boldsymbol{x}_T$ the centroid of T, with $0 < \alpha < 1/\ell$ such that K (respectively ∂K) is the image of T (respectively ∂T) by $\boldsymbol{\Xi}_T$. Since ∂K is an homothety of ∂T, any point $\boldsymbol{x}_{\partial T} \in \partial T$ and $\boldsymbol{x}_{\partial K} = \boldsymbol{\Xi}_T(\boldsymbol{x}_{\partial T}) \in \partial K$ share the same unit outward normal $\boldsymbol{n}$.

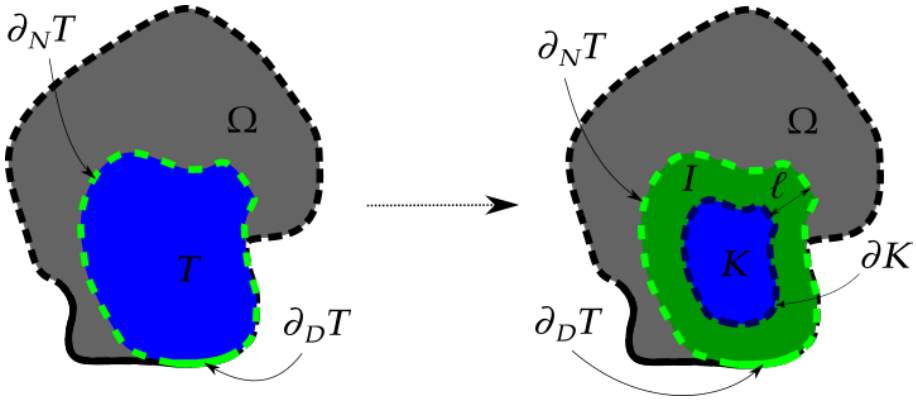

Figure 1. schematic representation of the composite region

3.3. Hu-Washizu on the interest zone

Le comportement du renfort K est caractérisé par le potentiel ψ_Ω, et il se déforme sous l'action of the body load $\boldsymbol{f}_V$. On note $\boldsymbol{u}_K \in U(K)$ le champ de déplacement, $\underset{\sim}{\boldsymbol{G}}_K \in G(K)$ le champs de gradient du déplacement et $\underset{\sim}{\boldsymbol{P}}_K \in S(K)$ les contraintes dans le renfort.

Le comportement de la matrice est défini par le potentiel ψ_I describing a linear elastic material of Young modulus $\beta(\ell/h_T)$ with a zero Poisson ratio such that

$$\psi_I = \frac{1}{2}\beta\frac{\ell}{h_T}\nabla\boldsymbol{u}_I : \nabla\boldsymbol{u}_I \tag{3}$$

where the dimensionless ratio ℓ/h_T balances the accumulated energy with the size of the domain T. La déplacement de la matrice $\boldsymbol{u}_I \in U(I)$ assure la continuité du déplacement entre les bords du domaine K et celui de T tel que

$$\boldsymbol{u}_I|_{\partial K} = \boldsymbol{u}_K|_{\partial K} \tag{4a}$$

$$\boldsymbol{u}_I|_{\partial T} = \boldsymbol{u}_{\partial T} \tag{4b}$$

On note $\underset{\sim}{\boldsymbol{G}}_I \in G(I)$ le gradient du champ de déplacement dans K and $\underset{\sim}{\boldsymbol{P}}_I \in S(I)$ les contraintes. Le pourtour de la matrice ∂T moves with a boundary displacement field $\boldsymbol{u}_{\partial T} \in V(\partial T)$, where $V(\partial T)$ denotes the space of kinematically admissible boundary displacements. The displacement at the boundary ∂T results from the interactions of ∂T with neighbouring media, *i.e.* from the action of $\Omega\backslash T$ onto ∂T or from some boundary condition.

Under such assumptions and by continuity of the traction force across ∂K, the Hu–Washizu functional over T writes

$$J_T^{HW} = \int_K \psi_\Omega + (\nabla_X\boldsymbol{u}_K - \underset{\sim}{\boldsymbol{G}}_K) : \underset{\sim}{\boldsymbol{P}}_K + \int_I \psi_I + (\nabla_X\boldsymbol{u}_I - \underset{\sim}{\boldsymbol{G}}_I) : \underset{\sim}{\boldsymbol{P}}_I - \int_K \boldsymbol{f}_V\cdot\boldsymbol{u}_K - \int_I \boldsymbol{f}_V\cdot\boldsymbol{u}_I - \int_{\partial_N T} \boldsymbol{t}_{\partial_N T}\cdot\boldsymbol{u}_{\partial T} \tag{5}$$

3.4. Interface description

Le comportement et la cinématique de notre zone composite connus, nous allons maintenant faire un certain nombre d'hypothèses sur l'expression des champs d'inconnues, en exploitant le fait que la matrice est de volume négligeable devant celui du renfort.

Since the interface I is thin compared to the cell volume T, let linearize the displacement in the interface I with respect to $\boldsymbol{n}$, such that

$$\boldsymbol{u}_I(\boldsymbol{x}) = \frac{\boldsymbol{u}_{\partial T}(\boldsymbol{m}_{\partial T}) - \boldsymbol{u}_K|_{\partial K}(\boldsymbol{m}_{\partial K})}{\ell} \otimes \boldsymbol{n}\cdot(\boldsymbol{x} - \boldsymbol{m}_{\partial K}) + \boldsymbol{u}_K|_{\partial K}(\boldsymbol{m}_{\partial K}) \tag{6}$$

where $\boldsymbol{m}_{\partial K} = \min_{\boldsymbol{x}_{\partial K}\in\partial K}\|\boldsymbol{x}_{\partial K} - \boldsymbol{x}\|$ and $\boldsymbol{m}_{\partial T} = \min_{\boldsymbol{x}_{\partial T}\in\partial T}\|\boldsymbol{x}_{\partial T} - \boldsymbol{x}\|$. That is, the displacement of the interface I linearly bridges that of the boundary ∂T to that of the bulk K.

Furthermore, let assume that $\underset{\sim}{\boldsymbol{P}}_I$ is constant along the direction $\boldsymbol{n}$ in I. By continuity of the traction force across ∂K, the following equality holds true

$$(\underset{\sim}{\boldsymbol{P}}_I - \underset{\sim}{\boldsymbol{P}}_K|_{\partial K})\cdot\boldsymbol{n} = 0 \quad \text{in} \quad I \tag{7}$$

3.5. Interface Hu-Washizu simplification

On donne en annexe Section 8 l'expression de (5) en exploitant les hypothèses faites Section 3.4 sur la forme des inconnues dans la matrice K. On montre en particulier que la fonctionelle (5) dépend de l'épaisseur de la matrice ℓ. Par la suite, en faisant tendre ℓ vers 0, on se rapproche du cadre discontinu, pour lequel le déplacement au bord du renfort est défini sur les bords de l'élement, mais n'est pas nécessairement égal à celui du contour de l'élément, étant donné l'existence d'une matrice infiniement fine. La formulation de l'énargie mécanqiue (5) qui découle de ce cas limite donne alors tous les ingrédients nécessaires à la définition des méthodes (hybrides) discontinues, et est donné par

$$\begin{aligned} J_T^{HW} = &\int_T \psi_\Omega + (\nabla \boldsymbol{u}_T - \underset{\sim}{\boldsymbol{G}}_T) : \underset{\sim}{\boldsymbol{P}}_T + \int_{\partial T} (\boldsymbol{u}_{\partial T} - \boldsymbol{u}_T|_{\partial T}) \cdot \underset{\sim}{\boldsymbol{P}}_T|_{\partial T} \cdot \boldsymbol{n} + \int_{\partial T} \frac{\beta}{2h_T} \|\boldsymbol{u}_{\partial T} - \boldsymbol{u}_T|_{\partial T}\|^2 \\ &- \int_T \boldsymbol{f}_V \cdot \boldsymbol{u}_T - \int_{\partial_N T} \boldsymbol{t}_{\partial_N T} \cdot \boldsymbol{u}_{\partial T} \end{aligned} \tag{8}$$

One notices that J_T^{HW} writes as a function of the four variables $(\boldsymbol{u}_T, \boldsymbol{u}_{\partial T}, \underset{\sim}{\boldsymbol{G}}_T, \underset{\sim}{\boldsymbol{P}}_T)$. Such an assumption relates to the concept of hybridization of the displacement unknown, which is at the foundation of Hybrid Discontinuous Galerkin methods. Indeed, the displacement of the solid is described by both a bulk and an interface displacement field, that might take different values on ∂T.

En outre, if the displacement is continuous at the boundary ∂T such that $\boldsymbol{u}_{\partial T}$ is the trace of the cell displacement $\boldsymbol{u}_T$ on ∂T and $\boldsymbol{u}_{\partial T} - \boldsymbol{u}_T|_{\partial T} = 0$, on retrouve le cadre continu et la fonctionnelle (**??**) for the three variables $(\boldsymbol{u}_T, \underset{\sim}{\boldsymbol{G}}_T, \underset{\sim}{\boldsymbol{P}}_T)$.

Besides, replacing $\boldsymbol{u}_{\partial T}$ by $\boldsymbol{u}_{T'}|_{\partial T}$ for any neighbouring cell T' to T amounts to describe the framework for Discontinuous Galerkin methods, where only the core unknown $\boldsymbol{u}_T$ is considered, and the displacement jump on ∂T depends on the trace of neighbouring cells displacement, instead of that only defined on the boundary.

Etant donné l'hybridization de l'inconnue primale, let introduce $U(\bar{T}) = U(T) \times V(\partial T)$ the space of all kinematically admissible bulk and boundary displacement pairs. On introduit également $U_0(\bar{T}) = U_0(T) \times V_0(\partial T)$ the sapce of all kinematically admissible bulk and boundary virtual displacement pairs, where $V_0(\partial T)$ denotes the space of kinematically admissible virtual displacement fields on the boundary ∂T.

3.6. Dérivation de la fonctionelle

La fonctionelle (8) définit le problème mixte sous forme faible, et revient à résoudre les problèmes couplés suivants

$$\frac{\partial J_T^{HW}}{\partial \boldsymbol{u}_T} \delta \boldsymbol{u}_T = \int_T \underset{\sim}{\boldsymbol{P}}_T : \nabla \delta \boldsymbol{u}_T - \int_T \boldsymbol{f}_V \cdot \delta \boldsymbol{u}_T - \int_{\partial T} \boldsymbol{\theta}_{\partial T} \cdot \delta \boldsymbol{u}_T|_{\partial T} \qquad \forall \delta \boldsymbol{u}_T \in U_0(T) \tag{9a}$$

$$\frac{\partial J_T^{HW}}{\partial \boldsymbol{u}_{\partial T}} \delta \boldsymbol{u}_{\partial T} = \int_{\partial_N T} (\boldsymbol{\theta}_{\partial T} - \boldsymbol{t}_{\partial_N T}) \cdot \delta \boldsymbol{u}_{\partial T} \qquad \forall \delta \boldsymbol{u}_{\partial T} \in V_0(\partial T) \tag{9b}$$

$$\frac{\partial J_T^{HW}}{\partial \underset{\sim}{\boldsymbol{G}}_T} \delta \underset{\sim}{\boldsymbol{G}}_T = \int_T (\frac{\partial \psi_\Omega}{\partial \underset{\sim}{\boldsymbol{G}}_T} - \underset{\sim}{\boldsymbol{P}}_T) : \delta \underset{\sim}{\boldsymbol{G}}_T \qquad \forall \delta \underset{\sim}{\boldsymbol{G}}_T \in G(T) \tag{9c}$$

$$\frac{\partial J_T^{HW}}{\partial \underset{\sim}{\boldsymbol{P}}_T} \delta \underset{\sim}{\boldsymbol{P}}_T = \int_T (\nabla \boldsymbol{u}_T - \underset{\sim}{\boldsymbol{G}}_T) : \delta \underset{\sim}{\boldsymbol{P}}_T + \int_{\partial T} (\boldsymbol{u}_{\partial T} - \boldsymbol{u}_T|_{\partial T}) \cdot \delta \underset{\sim}{\boldsymbol{P}}_T|_{\partial T} \cdot \boldsymbol{n} \qquad \forall \delta \underset{\sim}{\boldsymbol{P}}_T \in S(T) \tag{9d}$$

où on a introduit la *reconstructed traction force* $\boldsymbol{\theta}_{\partial T} = \underset{\sim}{\boldsymbol{P}}_T|_{\partial T} \cdot \boldsymbol{n} + (\beta/h_T)(\boldsymbol{u}_{\partial T} - \boldsymbol{u}_T|_{\partial T})$. In particular, (9a) is the expression of the principle of virtual works in T, where the *reconstructed traction force* $\boldsymbol{\theta}_{\partial T}$ replaces the usual expression $\underset{\sim}{\boldsymbol{P}}_T \cdot \boldsymbol{n}$ in the external contribution. (9b) denotes a supplementary equation to the usual continuous problem as described in (2), to account for the continuity of the flux $\boldsymbol{\theta}_{\partial T}$ across the cell boundary. La continuité du flux aux interfaces is indeed the tradeoff for having loosened la continuité du déplacement aux interfaces. (9c) accounts for the constitutive equation in a weak sense, and (9d) defines the equation of an enhanced gradient field, that does not reduce to the projection of $\nabla \boldsymbol{u}_T$ onto $G(T)$ as in (2c), since it is enriched by a boundary component that depends on the displacement jump, which is at the origin of the robustness of non-conformal methods to volumetric locking (see Section 8).

Instead of seeking the four fields explicitly, by noticing that minimization of (9d) defines a linear problem with any displacement pair $(\boldsymbol{v}_T, \boldsymbol{v}_{\partial T}) \in U(\bar{T})$, and that minimization of (9c) is linear with the derivative of ψ_Ω with respect to $\underset{\sim}{\boldsymbol{G}}_T$, one can eliminate (9c) and (9d) from the system, by considering the simplified functional (10) instead of (8)

$$J_T^{VW} = \int_T \psi_\Omega + \int_{\partial T} \frac{\beta}{2h_T} \|\boldsymbol{u}_{\partial T} - \boldsymbol{u}_T|_{\partial T}\|^2 - \int_T \boldsymbol{f}_V \cdot \boldsymbol{u}_T - \int_{\partial_N T} \boldsymbol{t}_{\partial_N T} \cdot \boldsymbol{u}_{\partial T} \tag{10}$$

Equation (9d) then results in the definition of the *reconstructed gradient* $\underset{\sim}{\boldsymbol{G}}_T(\boldsymbol{v}_T, \boldsymbol{v}_{\partial T})$ associated with any displacement pair $(\boldsymbol{v}_T, \boldsymbol{v}_{\partial T}) \in U(\bar{T})$ that solves

$$\int_T \underset{\sim}{\boldsymbol{G}}_T(\boldsymbol{v}_T, \boldsymbol{v}_{\partial T}) : \underset{\sim}{\tau}_T = \int_T \nabla \boldsymbol{v}_T : \underset{\sim}{\tau}_T + \int_{\partial T} (\boldsymbol{v}_{\partial T} - \boldsymbol{v}_T|_{\partial T}) \cdot \underset{\sim}{\tau}_T|_{\partial T} \cdot \boldsymbol{n} \quad \forall \underset{\sim}{\tau}_T \in S(T) \tag{11}$$

and the stress $\underset{\sim}{\boldsymbol{P}}_T(\underset{\sim}{\boldsymbol{G}}_T(\boldsymbol{v}_T, \boldsymbol{v}_{\partial T}))$ is defined as the projection onto $G(T)$ of the derivative of ψ_Ω with respect to $\underset{\sim}{\boldsymbol{G}}_T(\boldsymbol{v}_T, \boldsymbol{v}_{\partial T})$ for any displacement pair $(\boldsymbol{v}_T, \boldsymbol{v}_{\partial T}) \in U(\bar{T})$

$$\int_T \underset{\sim}{\boldsymbol{P}}_T : \underset{\sim}{\boldsymbol{\gamma}}_T = \int_T \frac{\partial \psi_\Omega}{\partial \underset{\sim}{\boldsymbol{G}}_T} : \underset{\sim}{\boldsymbol{\gamma}}_T \quad \forall \underset{\sim}{\boldsymbol{\gamma}}_T \in G(T) \tag{12}$$

In particular, one notices that (12) holds in a strong sense if $S(T) \subset G(T)$. The problem in primal form amounts to find the displacement pair $(\boldsymbol{u}_T, \boldsymbol{u}_{\partial T}) \in U(\bar{T})$ verifying $\boldsymbol{u}_{\partial T} = \boldsymbol{u}_D$ on $\partial_D T$, such that for all kinematically admissible displacements pairs $(\delta\boldsymbol{u}_T, \delta\boldsymbol{u}_{\partial T}) \in U_0(\bar{T})$, the functional (10) is minimal, *i.e.* such that

$$\delta J_{T,\text{int}}^{VW} - \delta J_{T,\text{ext}}^{VW} = 0 \tag{13}$$

with

$$\delta J_{T,\text{int}}^{VW} = \int_T \underset{\sim}{\boldsymbol{P}}_T(\underset{\sim}{\boldsymbol{G}}_T(\boldsymbol{u}_T, \boldsymbol{u}_{\partial T})) : \underset{\sim}{\boldsymbol{G}}_T(\delta\boldsymbol{u}_T, \delta\boldsymbol{u}_{\partial T}) + \int_{\partial T} (\beta/h_T) \boldsymbol{Z}_{\partial T}(\boldsymbol{u}_T, \boldsymbol{u}_{\partial T}) \cdot \boldsymbol{Z}_{\partial T}(\delta\boldsymbol{u}_T, \delta\boldsymbol{u}_{\partial T}) \tag{14a}$$

$$\delta J_{T,\text{ext}}^{VW} = \int_{\partial_N T} \boldsymbol{t}_{\partial_N T} \cdot \delta\boldsymbol{u}_{\partial T} + \int_T \boldsymbol{f}_V \cdot \delta\boldsymbol{u}_T \tag{14b}$$

where we introduced the jump function $\boldsymbol{Z}_{\partial T}$:

$$\boldsymbol{Z}_{\partial T}(\boldsymbol{v}_T, \boldsymbol{v}_{\partial T}) = \boldsymbol{v}_{\partial T} - \boldsymbol{v}_T|_{\partial T} \quad \forall (\boldsymbol{v}_T, \boldsymbol{v}_{\partial T}) \in U(\bar{T}) \tag{15}$$

In particular, one can readliy see the resemblance of (14) with (**??**), where the so called *reconstructed gradient* $\underset{\sim}{\boldsymbol{G}}_T(\boldsymbol{u}_T, \boldsymbol{u}_{\partial T})$ plays the role of the usual displacement Lagrangian gradient $\nabla \boldsymbol{u}_T$, and where an additional *stabilization term* corresponding to a traction energy on the boundary has been added to account for the penalization of the displacement jump on ∂T through $\boldsymbol{Z}_{\partial T}$ (or, equivalently, to account for the infinitésimale interface that lays between the bulk domain and its boundary). Equations (10), (11) and (12) define the mechanical problem to solve at the cell level for Hybrid Discontinuous Galerkin methods, and (13) describes the weak form of these equations.

3.7. Small strain

La formulation proposée en grandes déformations permet également un passage naturel au cadre des petites déformations. Dans ce contexte, étant donné que le gradient de la transformation $\underset{\sim}{\boldsymbol{F}}_T$ est supposé petit devant $\underset{\sim}{\mathbf{1}}$, on cherche le champ de déformation infinitésimale $\underset{\sim}{\boldsymbol{\varepsilon}}_T$ comme la formulation faible de $\nabla^s \boldsymbol{u}_T$ plutot que le gradient du champ de déplacement $\underset{\sim}{\boldsymbol{G}}_T$, et le tenseur des contraintes $\underset{\sim}{\boldsymbol{P}}_T$ est identifié à $\underset{\sim}{\boldsymbol{\sigma}}_T$, de sorte que le problème (8) devient

$$\begin{aligned} J_T^{HW} = &\int_T \psi_\Omega + (\nabla^s \boldsymbol{u}_T - \underset{\sim}{\boldsymbol{\varepsilon}}_T) : \underset{\sim}{\boldsymbol{\sigma}}_T + \int_{\partial T} (\boldsymbol{u}_{\partial T} - \boldsymbol{u}_T|_{\partial T}) \cdot \underset{\sim}{\boldsymbol{\sigma}}_T|_{\partial T} \cdot \boldsymbol{n} + \int_{\partial T} \frac{\beta}{2h_T} \|\boldsymbol{u}_{\partial T} - \boldsymbol{u}_T|_{\partial T}\|^2 \\ &- \int_T \boldsymbol{f}_V \cdot \boldsymbol{u}_T - \int_{\partial_N T} \boldsymbol{t}_{\partial_N T} \cdot \boldsymbol{u}_{\partial T} \end{aligned} \tag{16}$$

En poursuivant le même développement que précédemment, l'énargie à minimiser est donnée par l'équation 10 comme dans le cadre des grandes déformations. En revanche,l'équation du gradient reconstruit 11 devient

$$\int_T \underset{\sim}{\boldsymbol{\varepsilon}}_T(\boldsymbol{v}_T, \boldsymbol{v}_{\partial T}) : \underset{\sim}{\boldsymbol{\tau}}_T = \int_T \nabla^s \boldsymbol{v}_T : \underset{\sim}{\boldsymbol{\tau}}_T + \int_{\partial T} (\boldsymbol{v}_{\partial T} - \boldsymbol{v}_T|_{\partial T}) \cdot \underset{\sim}{\boldsymbol{\tau}}_T|_{\partial T} \cdot \boldsymbol{n} \quad \forall \underset{\sim}{\boldsymbol{\tau}}_T \in S(T) \tag{17}$$

En particulier, les deformations $\underset{\sim}{\boldsymbol{\varepsilon}}_T$ étant symétriques, tout comme la contrainte $\underset{\sim}{\boldsymbol{\sigma}}_T$, on cherche donc ces grandeurs dans l'espace des déformations $G(T)$ et contraintes $S(T)$ statiquement admissbles et symétriques. L'expression de la contrainte en fonction de la déformation de cellule est alors donnée par

$$\int_T \underset{\sim}{\boldsymbol{\sigma}}_T : \underset{\sim}{\boldsymbol{\gamma}}_T = \int_T \frac{\partial \psi_\Omega}{\partial \underset{\sim}{\boldsymbol{\varepsilon}}_T} : \underset{\sim}{\boldsymbol{\gamma}}_T \quad \forall \underset{\sim}{\boldsymbol{\gamma}}_T \in G(T) \tag{18}$$

4. Discretization

On a décrit section précédente le problème faible pour un élément dit composite, aboutissant à une formulation faisant intervenir le éplcament de l'élement mais aussi celui de son enveloppe, par l'introduction d'une vanishing interface. Dans la présente section, on définit le problème gloabl à réésoudre sur l'ensemble de la structure. On la suppose composée de ces éléments composites, de sorte qu'on est amené à définir le squelette du maillage, c'est à dire le support de l'ensemble des déplacement des faces des éléments.

On considère que Ω est discrétisé par un maillage composé de cellules convexes, polyhédriques, et à faces planes. Les cellules du maillages sont regroupées dans l'ensemble $\mathcal{T}(\Omega) = \{T_i \subset \Omega \mid 1 \leq i \leq N_T\}$, où N_T désigne le nombre de cellules. On introduit ensuite $\mathcal{F}(\Omega) = \{F_i \subset \Omega \mid 1 \leq i \leq N_F\}$ the skeleton of the mesh, collecting all element faces F_i in the mesh, where N_F denotes the number of faces in the mesh. En particulier, two elements sharing a boundary also share the same boundary unknown, *i.e.* for any $(T, T') \in \mathcal{T}(\Omega)$ such that $\partial T \cap \partial T' \neq \emptyset$, there is $\boldsymbol{u}_{\partial T \cap \partial T'} = \boldsymbol{u}_{\partial T' \cap \partial T}$.

A face F is a subset of Ω, and either there are two cells T and T' such that $F = \partial T \cap \partial T'$ (F is then an interior face), or there is a single cell T such that $F = \partial T \cap \partial \Omega$ (F is then an exterior face). Let $\mathcal{F}^i(\Omega)$ denote the set of interior faces, and $\mathcal{F}^e(\Omega)$ that of exterior ones. $\mathcal{F}^e(\Omega)$ is partitioned into $\mathcal{F}^e_D(\Omega) = \{F \in \mathcal{F}^e(\Omega) \mid F \subset \partial_D \Omega\}$ the set of exterior faces imposed to prescribed Dirichlet boundary conditions, and into $\mathcal{F}^e_N(\Omega) = \{F \in \mathcal{F}^e(\Omega) \mid F \subset \partial_N \Omega\}$ the set of exterior faces imposed to prescribed Neumann boundary conditions. Similarly, for any element $T \in \mathcal{T}$, let $\mathcal{F}(T) = \{F \in \mathcal{F} \mid F \subset \partial T\}$ the set of faces composing the boundary of T. The composition of both $\mathcal{T}(\Omega)$ and $\mathcal{F}(\Omega)$ forms the hybrid mesh $\bar{\mathcal{T}}(\Omega) = \{\mathcal{T}(\Omega), \mathcal{F}(\Omega)\}$.

Contrary to the standard finite element method that consists in seeking a global solution in a regular enough space over the whole mesh, we consider here a much broader space that consists in $U(\mathcal{T}) = \prod_{T \in \mathcal{T}(\Omega)} U(T)$ the collection of all regular enough displacements element-wise. Similarly, we consider $V(\mathcal{F}) = \prod_{F \in \mathcal{F}(\Omega)} V(F)$ the space of all regular enough displacements face-wise for the skeleton unknown, such that the global solution space $U(\bar{\mathcal{T}}) = U(\mathcal{T}) \times V(\mathcal{F})$ for the whole problem is simply the assembly of all element and face spaces in the mesh.

Let then $(\boldsymbol{v}_\mathcal{T}, \boldsymbol{v}_\mathcal{F}) \in U(\bar{\mathcal{T}})$ a displacement pair in the global functional space such that for each $T \in \mathcal{T}(\Omega), \boldsymbol{v}_\mathcal{T} = \boldsymbol{v}_T$ in T and for each $F \in \mathcal{F}(\Omega), \boldsymbol{v}_\mathcal{F} = \boldsymbol{v}_F$ on F, where $\boldsymbol{v}_T \in U(T)$ and $\boldsymbol{v}_F \in V(\partial T)$ denote a cell and a face displacement field respectively. With obvious notations, let $U_0(\mathcal{T})$ the space of global kinematically admissible virtual cell displacement fields in $\mathcal{T}(\Omega)$, $V_0(\mathcal{F})$ that of global kinematically admissible virtual face displacement fields in $\mathcal{F}(\Omega)$ and $U_0(\bar{\mathcal{T}})$ that of kinematically admissible virtual global displacement pairs in $\bar{\mathcal{T}}(\Omega)$.

The weak form of the global mechanical problem of Ω reads : find the global displacement unknown pair $(\boldsymbol{u}_\mathcal{T}, \boldsymbol{u}_\mathcal{F}) \in U(\bar{\mathcal{T}})$ verifying $\boldsymbol{u}_\mathcal{F}|_{\partial_D \Omega} = \boldsymbol{u}_D$ on $\partial_D \Omega$ such that $\forall (\delta \boldsymbol{u}_\mathcal{T}, \delta \boldsymbol{u}_\mathcal{F}) \in U_0(\bar{\mathcal{T}})$

$$\delta J^{VW}_{\mathcal{T},\text{int}} - \delta J^{HW}_{\mathcal{T},\text{ext}} = 0 \tag{19}$$

with

$$\delta J^{VW}_{\mathcal{T},\text{int}} = \sum_{T \in \mathcal{T}(\Omega)} \int_T \underset{\sim}{\boldsymbol{P}}_T(\underset{\sim}{\boldsymbol{G}}_T(\boldsymbol{u}_T, \boldsymbol{u}_{\partial T})) : \underset{\sim}{\boldsymbol{G}}_T(\delta \boldsymbol{u}_T, \delta \boldsymbol{u}_{\partial T}) + \int_{\partial T} (\beta / h_T) \boldsymbol{Z}_{\partial T}(\boldsymbol{u}_T, \boldsymbol{u}_{\partial T}) \cdot \boldsymbol{Z}_{\partial T}(\delta \boldsymbol{u}_T, \delta \boldsymbol{u}_{\partial T}) \tag{20a}$$

$$\delta J^{HW}_{\mathcal{T},\text{ext}} = \sum_{F \in \mathcal{F}^e_N(\Omega)} \int_F \boldsymbol{t}_N \cdot \delta \boldsymbol{u}_F + \sum_{T \in \mathcal{T}(\Omega)} \int_T \boldsymbol{f}_V \cdot \delta \boldsymbol{u}_T \tag{20b}$$

where for each element $T \in \mathcal{T}(\Omega)$, the boundary displacement field $\boldsymbol{v}_{\partial T}$ is such that $\boldsymbol{v}_{\partial T} = \boldsymbol{v}_F$ on F for every $F \in \mathcal{F}(T)$, and the displacement space in the boundary $V(\partial T)$ is the collection of displacement spaces in faces composing it such that $V(\partial T) = \prod_{F\in\mathcal{F}(T)} V(F)$.

A polynomial approximation of the global solution is then sought in a subspace of $U(\mathcal{T})$, and for each element $T \in \mathcal{T}(\Omega)$, we denote $U^h(T) \subset U(T)$ the approximation displacement space in the cell, and $V^h(\partial T) \subset V(\partial T)$ that on the boundary. Moreover, though they are not primal unknowns of the problem, one need to define $G^h(T) \subset G(T)$ the space used to build the discrete reconstructed gradient and $S^h(T) \subset S(T)$ that chosen for the discrete stress such that

$$\begin{aligned} U^h(T) &= P^l(T, \mathbb{R}^d) \\ V^h(\partial T) &= P^k(\partial T, \mathbb{R}^d) \\ G^h(T) &= P^k(T, \mathbb{R}^{d\times d}) \\ S^h(T) &= P^k(T, \mathbb{R}^{d\times d}) \end{aligned}$$

where the cell displacement polynomial order l might be chosen different from the face displacement order k such that $k-1 \leq l \leq k+1$. Accounting for the possible different polynomial order between the cell and faces, one can specify a discrete jump function in a natural way such that it delivers the displacement difference point-wise for any displacement pair $(\boldsymbol{v}_T^l, \boldsymbol{v}_{\partial T}^k) \in U^h(\bar{T})$

$$\boldsymbol{Z}_{\partial T}^{HDG}(\boldsymbol{v}_T^l, \boldsymbol{v}_{\partial T}^k) = \Pi_{\partial T}^k(\boldsymbol{v}_{\partial T}^k - \boldsymbol{v}_T^l|_{\partial T}) \tag{21}$$

where $U^h(\bar{T}) = U^h(T) \times V^h(\partial T)$ and $\Pi_{\partial T}^k$ denotes the orthogonal projector onto $V^h(\partial T)$. This straightforward discrete jump function is at the origin of Hybrid Discontinuous Galerkin methods, and grants a convergence of order k in the energy norm. A richer discrete jump function $\boldsymbol{Z}_{\partial T}^{HHO}$ providing a convergence of order $k+1$ in the energy norm was introduced in [2], hence giving the Hybrid High Order method its name, such that

$$\boldsymbol{Z}_{\partial T}^{HHO}(\boldsymbol{v}_T^l, \boldsymbol{v}_{\partial T}^k) = \Pi_{\partial T}^k(\boldsymbol{v}_{\partial T}^k - \boldsymbol{v}_T^l|_{\partial T} - ((I_T^{k+1} - \Pi_T^k)(\boldsymbol{w}_T^{k+1}))|_{\partial T}) \tag{22}$$

where Π_T^k is the projector onto $P^k(T, \mathbb{R}^d)$, I_T^{k+1} is the identity function in $D^h(T) = P^{k+1}(T, \mathbb{R}^d)$, and $\boldsymbol{w}_T^{k+1} \in D^h(T)$ denotes a higher order discrete displacement solving the following linear problem for any displacement pair $(\boldsymbol{v}_T^l, \boldsymbol{v}_{\partial T}^k) \in U^h(\bar{T})$

$$\int_T \nabla \boldsymbol{w}_T^{k+1} : \nabla \boldsymbol{d}_T^{k+1} = \int_T \nabla \boldsymbol{v}_T^l : \nabla \boldsymbol{d}_T^{k+1} + \int_{\partial T} (\boldsymbol{v}_{\partial T}^k - \boldsymbol{v}_T^l) \cdot \nabla \boldsymbol{d}_T^{k+1} \cdot \boldsymbol{n} \qquad \forall \boldsymbol{d}_T^{k+1} \in D^h(T) \tag{23a}$$

$$\int_T \boldsymbol{w}_T^{k+1} = \int_T \boldsymbol{v}_T^l \tag{23b}$$

Let $U^h(\mathcal{T}) = \prod_{T\in\mathcal{T}(\Omega)} U^h(T)$ the global discrete cell displacement space, $V^h(\mathcal{F}) = \prod_{F\in\mathcal{F}(\Omega)} V^h(F)$ the global discrete face displacement space, and $U^h(\bar{\mathcal{T}}) = U^h(\mathcal{T}) \times V^h(\mathcal{F})$ the global unknown approximation space. Let $U_0^h(\mathcal{T})$ and $V_0^h(\mathcal{F})$ the respective discrete mesh and skeleton virtual displacement spaces, and $U_0^h(\bar{\mathcal{T}}) = U_0^h(\mathcal{T}) \times V_0^h(\mathcal{F})$ the discrete virtual global displacement space.

The global mechanical problem in discrete weak form for the Hybrid High Order method finally writes : find the global displacement unknown pair $(\boldsymbol{u}_{\mathcal{T}}^l, \boldsymbol{u}_{\mathcal{F}}^k) \in U^h(\bar{\mathcal{T}})$ verifying $\boldsymbol{u}_{\mathcal{F}}^k|_{\partial_D\Omega} = \boldsymbol{u}_D$ on $\partial_D\Omega$ such that $\forall(\delta\boldsymbol{u}_{\mathcal{T}}^l, \delta\boldsymbol{u}_{\mathcal{F}}^k) \in U_0^h(\bar{\mathcal{T}})$

$$\delta J_{\mathcal{T},\text{int}}^{HHO} - \delta J_{\mathcal{T},\text{ext}}^{HHO} = 0 \tag{24}$$

with

$$\delta J_{\mathcal{T},\text{int}}^{HHO} = \sum_{T\in\mathcal{T}(\Omega)} \int_T \underset{\sim}{\boldsymbol{P}}_T^k(\underset{\sim}{\boldsymbol{G}}_T^k(\boldsymbol{u}_T^l, \boldsymbol{u}_{\partial T}^k)) : \underset{\sim}{\boldsymbol{G}}_T^k(\delta\boldsymbol{u}_T^l, \delta\boldsymbol{u}_{\partial T}^k) + \int_{\partial T} (\beta/h_T) \boldsymbol{Z}_{\partial T}^{HHO}(\boldsymbol{u}_T^l, \boldsymbol{u}_{\partial T}^k) \cdot \boldsymbol{Z}_{\partial T}^{HHO}(\delta\boldsymbol{u}_T^l, \delta\boldsymbol{u}_{\partial T}^k) \tag{25a}$$

$$\delta J_{\mathcal{T},\text{ext}}^{HHO} = \sum_{F\in\mathcal{F}_N^e(\Omega)} \int_F \boldsymbol{t}_N \cdot \delta\boldsymbol{u}_F^k + \sum_{T\in\mathcal{T}(\Omega)} \int_T \boldsymbol{f}_V \cdot \delta\boldsymbol{u}_T^l \tag{25b}$$

with the discrete reconstructed gradient $\underset{\sim}{\boldsymbol{G}}_T^k(\boldsymbol{v}_T^l, \boldsymbol{v}_{\partial T}^k) \in G^h(T)$ solving $\forall(\boldsymbol{v}_T^l, \boldsymbol{v}_{\partial T}^k) \in U^h(\bar{T})$

$$\int_T \underset{\sim}{\boldsymbol{G}}_T^k(\boldsymbol{v}_T^l, \boldsymbol{v}_{\partial T}^k) : \underset{\sim}{\boldsymbol{\tau}}_T^k = \int_T \nabla \boldsymbol{v}_T^l : \underset{\sim}{\boldsymbol{\tau}}_T^k + \int_{\partial T} (\boldsymbol{v}_{\partial T}^k - \boldsymbol{v}_T^l|_{\partial T}) \cdot \underset{\sim}{\boldsymbol{\tau}}_T^k|_{\partial T} \cdot \boldsymbol{n} \quad \forall \underset{\sim}{\boldsymbol{\tau}}_T^k \in S^h(T) \tag{26}$$

5. A HHO method for the axi-symmetric framework

In the following section, we derive a Hybrid High order method for an axi-symmetric framework. The cartesian space is expressed in cylindrical coordinates and a point $\boldsymbol{x} \in \Omega$ has coordinates $\boldsymbol{x} = (r, z, \theta)$ where r denotes the radial component, z the ordinate one, and θ is the angular component describing a revolution around the axis $r = 0$. By cylindrical symmetry, the angular displacement u_θ is supposed to be zero, and both components u_r and u_z do not depend on the angular coordinate θ. Adopting notations introduced in Section 3, let T an open subset of $\Omega \subset \mathbb{R}^2$ in the (r, z) plane with cell displacement $\boldsymbol{u}_T \in U(T)$ and boundary displacement $\boldsymbol{u}_{\partial T} \in V(\partial T)$. The partial derivatives of $\boldsymbol{u}_T$ with respect to the cylindrical coordinates are given by :

$$\forall i, j \in \{r, z\}, u_{Ti,j} = \frac{\partial u_{Ti}}{\partial j} \quad \text{and} \quad u_{T\theta,\theta} = \frac{u_{Tr}}{r} \tag{27}$$

In order to express a Hybrid High Order method in such a framework and owing to the assumptions on the displacement and its gradient, the definition of the reconstructed gradient (11) needs be modified accordingly, and the angular component $G_{T\theta\theta}$ does not define by the same equation as those in the other directions. In particular, for any displacement pair $(\boldsymbol{v}_T, \boldsymbol{v}_{\partial T}) \in U(T) \times V(\partial T)$, the component $G_{T\theta\theta}(v_{Tr}, v_{\partial Tr})$ solves

$$\int_T 2\pi r G_{T\theta\theta}(v_{Tr}, v_{\partial Tr})\tau_{T\theta\theta} = \int_T 2\pi r \frac{u_{Tr}}{r}\tau_{T\theta\theta} = \int_T 2\pi u_{Tr}\tau_{T\theta\theta} \quad \forall \underset{\sim}{\tau}_T \in S(T) \tag{28}$$

whereas in the radial and ordonal directions, *i.e.* $\forall i, j \in \{r, z\}$, the expression given in (11) is retrieved, and the component $G_{Tij}(v_{Ti}, v_{\partial Ti})$ solves :

$$\int_T 2\pi r G_{Tij}(v_{Ti}, v_{\partial Ti})\tau_{Tij} = \int_T 2\pi r \frac{\partial u_{Ti}}{\partial j}\tau_{ij} - \int_{\partial T} 2\pi r (u_{\partial Ti} - u_{Ti}|_{\partial T})\tau_{Tij}|_{\partial T} n_j \quad \forall \underset{\sim}{\tau}_T \in S(T) \tag{29}$$

As for the reconstructed gradient, the higher order potential term needed to define the HHO jump function needs also be reconsidered such that $\forall \boldsymbol{d}_T^{k+1} \in D^h(T)$, the radial component w_{Tr}^{k+1} solves

$$\begin{aligned}\int_T 2\pi r \Big(\sum_{i\in\{r,z\}} \frac{\partial w_{Tr}^{k+1}}{\partial i}\frac{\partial d_{Tr}^{k+1}}{\partial i} + \frac{w_{Tr}^{k+1}}{r}\frac{d_{Tr}^{k+1}}{r} \Big) = \int_T 2\pi r \Big(\sum_{i\in\{r,z\}} \frac{\partial u_{Tr}}{\partial i}\frac{\partial d_{Tr}^{k+1}}{\partial i} + \frac{u_{Tr}}{r}\frac{d_{Tr}^{k+1}}{r} \Big) \\ + \int_{\partial T} 2\pi r \sum_{i\in\{r,z\}} (u_{\partial Tr} - u_{Tr}|_{\partial T}) \frac{\partial d_{Tr}^{k+1}}{\partial i}|_{\partial T} n_i\end{aligned} \tag{30}$$

and the ordinate component w_{Tz}^{k+1} solves :

$$\int_T 2\pi r \sum_{i\in\{r,z\}} \frac{\partial w_{Tz}^{k+1}}{\partial i}\frac{\partial d_{Tz}^{k+1}}{\partial i} = \int_T 2\pi r \sum_{i\in\{r,z\}} \frac{\partial u_{Tz}}{\partial i}\frac{\partial d_{Tz}^{k+1}}{\partial i} - \int_{\partial T} 2\pi r \sum_{i\in\{r,z\}} (u_{\partial Tz} - u_{Tz}|_{\partial T}) \frac{\partial d_{Tz}^{k+1}}{\partial i}|_{\partial T} n_i \tag{31a}$$

$$\int_T 2\pi r w_{Tz}^{k+1} = \int_T 2\pi r u_{Tz} \tag{31b}$$

In particular, one notices that the mean value condition is not needed on the radial component of the higher order displacement since the left hand side of the system described by (30) depends directly on the displacement unknown and not only on its gradient as in (31).

Moreover, since in cylindrical coordinates, all integrals depend on the radial component r, there is a singularity at $r = 0$ for boundary integrals on faces located on the symmetry axis, and from a geometrical standpoint, these faces lose a dimension; a face that is not located on the symmetry axis behaves like a shell by revolution of the (r, z) plane, whereas one attached to the axis reduces to a beam that is only allowed to move and morph in the z direction. On a more algebraic note, the problem as such is ill-defined, since building the jump function involves inverting a mass matrix in $V^h(\partial T)$ to define the projector $\Pi_{\partial T}^k$. Therefore, a face on the axis is swelled by a small radius ϱ such that it becomes a cylinder with same dimensions as the others (see Figure 2)

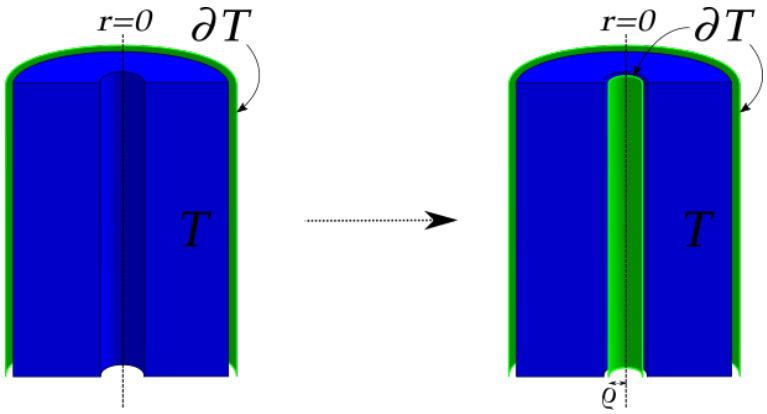

Figure 2. schematic representation of the modeling of a face located on the symmetry axis

6. Implementation

Let Q_T a quadrature of T of order at least $2k$. In the following, the expression $\{\cdot\}$ denotes a real-valued vector, and the notation $[\cdot]$ a real-valued matrix. From an algebraic standpoint, (26) defines a linear problem consisting in inverting a mass matrix in $G^h(T)$ in order to obtain $[B_T]$ the discrete gradient operator acting on the pair $(\boldsymbol{v}_T^l, \boldsymbol{v}_T^k)$ at a quadrature point $\boldsymbol{x}_q \in Q_T$, such that the algebraic realization of (26) reads

$$\left\{\underset{\sim}{\boldsymbol{G}}_T^k(\boldsymbol{v}_T^l, \boldsymbol{v}_{\partial T}^k)\right\}(\boldsymbol{x}_q) = \begin{bmatrix} B_T & B_{\partial T} \end{bmatrix}(\boldsymbol{x}_q) \cdot \begin{Bmatrix} \boldsymbol{v}_T^l \\ \boldsymbol{v}_{\partial T}^k \end{Bmatrix} \quad \forall (\boldsymbol{v}_T^l, \boldsymbol{v}_{\partial T}^k) \in U^h(\bar{T}) \tag{32}$$

where we have decomposed the expression of the discrete gradient operator $[B_T]$ into a cell block B_T and a boundary block $B_{\partial T}$, to emphasize the dependence of the problem on both unknowns. Similarly, the algebraic realization of (22) amounts to compute the stabilization operator $[Z_T]$ such that

$$\left\{\boldsymbol{Z}_{\partial T}^{HHO}(\boldsymbol{v}_T^l, \boldsymbol{v}_{\partial T}^k)\right\} = \begin{bmatrix} Z_T & Z_{\partial T} \end{bmatrix} \cdot \begin{Bmatrix} \boldsymbol{v}_T^l \\ \boldsymbol{v}_{\partial T}^k \end{Bmatrix} \quad \forall (\boldsymbol{v}_T^l, \boldsymbol{v}_{\partial T}^k) \in U^h(\bar{T}) \tag{33}$$

Since (26) and (22) depend on the geometry of the element T only, one can compute the operators $[B_T]$ and $[Z_T]$ for each element once and for all in an offline pre-computation step by working in the reference configuration. Once this offline step is performed, the algebraic form of the problem resembles closely to the standard finite element one, where the operator $[B_T]$ replaces the usual shape function gradient operator, and the stabilization operator $[Z_T]$ is incorporated in the expression of the tangent matrix and in that of internal forces.

In the following, let $(\boldsymbol{u}_T^{l,m,n}, \boldsymbol{u}_{\partial T}^{k,m,n})$ denote the displacement pair value at some pseudo time step m and some iteration n. The initial value of the displacement at time step $m = 0$ and iteration $n = 0$ is set to zero, and at a new pseudo time step $m + 1$, the displacement at the first iteration $n = 0$ takes the value of the displacement of the last iteration of the previous time step. In such a context, the internal forces vector $\{F_T^{int}(\boldsymbol{u}_T^{l,m,n}, \boldsymbol{u}_{\partial T}^{k,m,n})\}$ writes

$$\begin{aligned} \left\{F_T^{int}(\boldsymbol{u}_T^{l,m,n}, \boldsymbol{u}_{\partial T}^{k,m,n})\right\} = \sum_{\boldsymbol{x}_q \in Q_T} & \begin{bmatrix} B_T & B_{\partial T} \end{bmatrix}^{\text{trans}}(\boldsymbol{x}_q) \cdot \left\{\underset{\sim}{\boldsymbol{P}}_T^k(\underset{\sim}{\boldsymbol{G}}_T^k(\boldsymbol{u}_T^{l,m,n}, \boldsymbol{u}_{\partial T}^{k,m,n}))\right\}(\boldsymbol{x}_q) \\ & + \beta \begin{bmatrix} Z_T & Z_{\partial T} \end{bmatrix}^{\text{trans}} \cdot \begin{bmatrix} Z_T & Z_{\partial T} \end{bmatrix} \cdot \begin{Bmatrix} \boldsymbol{u}_T^{l,m,n} \\ \boldsymbol{u}_{\partial T}^{k,m,n} \end{Bmatrix} \end{aligned} \tag{34}$$

where the superscript $[\cdot]^{\text{trans}}$ denotes the transpose operation, and $\{\underset{\sim}{\boldsymbol{P}}_T^k(\underset{\sim}{\boldsymbol{G}}_T^k(\boldsymbol{u}_T^{l,m,n}, \boldsymbol{u}_{\partial T}^{k,m,n}))\}$ is the stress components vector, computed by integration of the behavior law at each quadrature point $\boldsymbol{x}_q$ from the values of the displacement gradient $\underset{\sim}{\boldsymbol{G}}_T^k(\boldsymbol{u}_T^{l,m,n}, \boldsymbol{u}_{\partial T}^{k,m,n})$. The external forces vector is, as is customary with the standard finite element method,

the evaluation of the given bulk and boundary loads at respective cell and face quadrature points tested against the respective cell and face shape functions, and is denoted

$$\left\{F_T^{ext}\right\} = \begin{Bmatrix} \boldsymbol{f}_V \\ \boldsymbol{t}_N \end{Bmatrix} \tag{35}$$

The tangent matrix $[K_T^{tan}(\boldsymbol{u}_T^{l,m,n}, \boldsymbol{u}_{\partial T}^{k,m,n})]$ is the sum of the usual product of the displacement gradients by the tangent operator $\underset{\approx}{\boldsymbol{A}}(\boldsymbol{u}_T^{l,m,n}, \boldsymbol{u}_{\partial T}^{k,m,n})$ and of an additional stabilization term such that

$$\begin{aligned} \left[K_T^{tan}(\boldsymbol{u}_T^{l,m,n}, \boldsymbol{u}_{\partial T}^{k,m,n})\right] = \sum_{\boldsymbol{x}_q \in Q_T} & \left[B_T \qquad B_{\partial T}\right]^{\text{trans}}(\boldsymbol{x}_q) \cdot \left[\underset{\approx}{\boldsymbol{A}}(\boldsymbol{u}_T^{l,m,n}, \boldsymbol{u}_{\partial T}^{k,m,n})\right](\boldsymbol{x}_q) \cdot \left[B_T \qquad B_{\partial T}\right](\boldsymbol{x}_q) \\ & + \beta \left[Z_T \qquad Z_{\partial T}\right]^{\text{trans}} \cdot \left[Z_T \qquad Z_{\partial T}\right] \end{aligned} \tag{36}$$

where $\underset{\approx}{\boldsymbol{A}}(\boldsymbol{u}_T^{l,m,n}, \boldsymbol{u}_{\partial T}^{k,m,n})$ is the derivative of the stress with respect to the displacement gradient

$$\underset{\approx}{\boldsymbol{A}}(\boldsymbol{u}_T^{l,m,n}, \boldsymbol{u}_{\partial T}^{k,m,n}) = \frac{\partial \underset{\sim}{\boldsymbol{P}}_T^k}{\partial \underset{\sim}{\boldsymbol{G}}_T^k} \tag{37}$$

Following the iterative Newton method, the algebraic system to solve at the element level consists in finding the displacement increment $(\delta \boldsymbol{u}_T^l, \delta \boldsymbol{u}_{\partial T}^k)$ that solves

$$-\left[K_T^{tan}(\boldsymbol{u}_T^{l,m,n}, \boldsymbol{u}_{\partial T}^{k,m,n})\right] \cdot \begin{Bmatrix} \delta \boldsymbol{u}_T^l \\ \delta \boldsymbol{u}_{\partial T}^k \end{Bmatrix} = \left\{F_T^{int}(\boldsymbol{u}_T^{l,m,n}, \boldsymbol{u}_{\partial T}^{k,m,n})\right\} - \left\{F_T^{ext}\right\} = \left\{R_T^{m,n}\right\} \tag{38}$$

In particular, since both $[B_T]$ and $[Z_T]$ are expressed in terms of cell and boundary blocks, so does the tangent matrix which can be decomposed into four coupled cell-boundary blocks with the notation

$$\left[K_T^{tan}(\boldsymbol{u}_T^{l,m,n}, \boldsymbol{u}_{\partial T}^{k,m,n})\right] = \begin{bmatrix} K_{TT}(\boldsymbol{u}_T^{l,m,n}, \boldsymbol{u}_{\partial T}^{k,m,n}) & K_{T\partial T}(\boldsymbol{u}_T^{l,m,n}, \boldsymbol{u}_{\partial T}^{k,m,n}) \\ K_{\partial TT}(\boldsymbol{u}_T^{l,m,n}, \boldsymbol{u}_{\partial T}^{k,m,n}) & K_{\partial T\partial T}(\boldsymbol{u}_T^{l,m,n}, \boldsymbol{u}_{\partial T}^{k,m,n}) \end{bmatrix} \tag{39}$$

Moreover, since $\underset{\approx}{\boldsymbol{A}}(\boldsymbol{u}_T^{l,m,n}, \boldsymbol{u}_{\partial T}^{k,m,n})$ is definite symmetric (and positive until an eventual loss of coercivity for *e.g.* high plastic deformations), the cell block K_{TT} is invertible and one can condensate it through a Schur complement step in order to eliminate the cell unknown, such that (38) expresses only in terms of boundary increment unknowns

$$-\left[K_T^{tan}(\boldsymbol{u}_T^{l,m,n}, \boldsymbol{u}_{\partial T}^{k,m,n})\right]_{\text{cond}} \cdot \left\{\delta \boldsymbol{u}_{\partial T}^k\right\} = \left\{F_T^{int}(\boldsymbol{u}_T^{l,m,n}, \boldsymbol{u}_{\partial T}^{k,m,n})\right\}_{\text{cond}} - \left\{F_T^{ext}\right\}_{\text{cond}} = \left\{R_T^{m,n}\right\}_{\text{cond}} \tag{40}$$

with

$$\left[K_T^{tan}\right]_{\text{cond}} = \left[K_{\partial T\partial T}\right] - \left[K_{\partial TT}\right] \cdot \left[K_{TT}\right]^{-1} \cdot \left[K_{T\partial T}\right] \quad \text{and} \quad \left\{R_T\right\}_{\text{cond}} = \left\{R_{\partial T}\right\} - \left[K_{\partial TT}\right] \cdot \left[K_{TT}\right]^{-1} \cdot \left\{R_T\right\} \tag{41}$$

The incremental cell displacement expresses linearly with the respect to the boundary one such that

$$\left\{\delta \boldsymbol{u}_T^l\right\} = \left[K_{TT}\right]^{-1} \left(-\left\{R_T\right\} - \left[K_{T\partial T}\right] \cdot \left\{\delta \boldsymbol{u}_{\partial T}^k\right\}\right) \tag{42}$$

A schematic representation of an Newton iteration is given in Figure 3

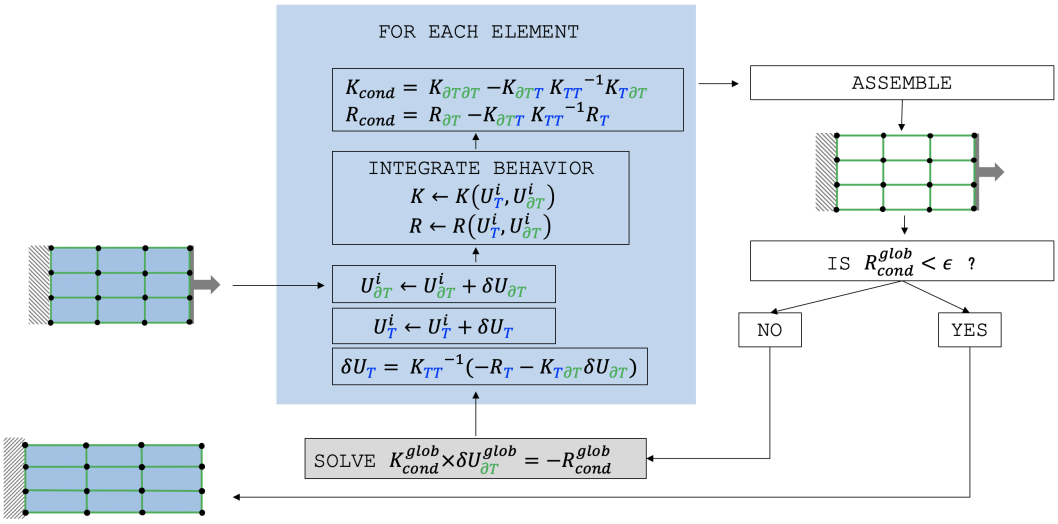

Figure 3. Description schématique de l'algorithme de condensation statique

6.1. Résolution par équilibre de cellule

We propose an alternative to the static condensation solving algorithm, postulating an implicit relation between the increment of the cell unknowns and the increment of the faces, and consisting in solving locally a nonlinear system on the cell increment with a fixed face increment, in order to check the equilibrium of the cell with its faces at each iteration of the global problem. This new solution scheme is described in Figure 4, where we note i a Newton iteration for solving the global problem on the set of face unknowns, and j a Newton iteration for solving the local problem on the cell unknowns in an element.

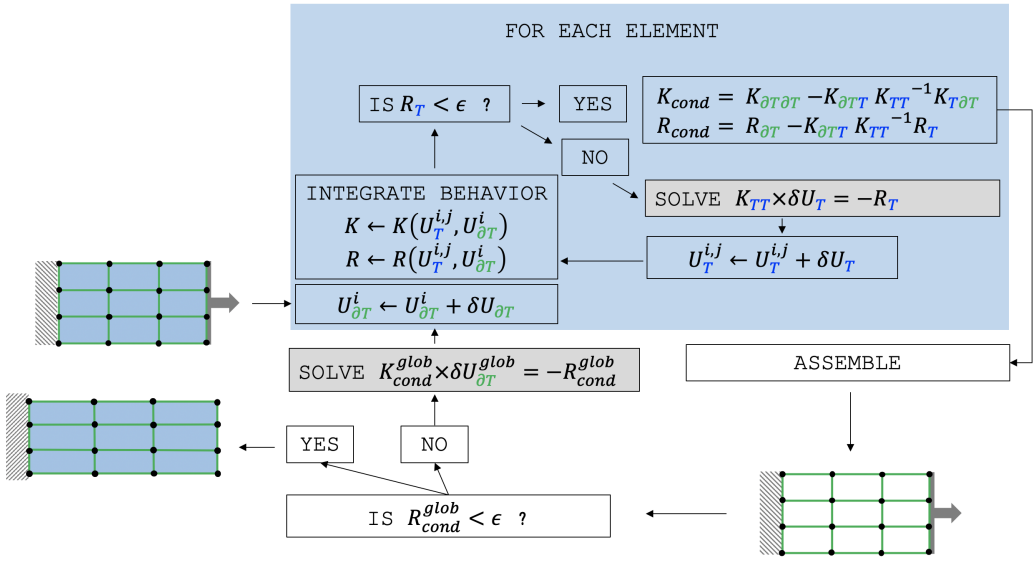

Figure 4. Description schématique de l'algorithme d'équilibre de cellule

7. Numerical examples

The goal of this section is to evaluate the proposed HHO method on benchmarks from the literature: (i) a necking of a 2D notched bar subjected to uniaxial extension, (ii) a quasi-incompressible sphere under internal pressure. We

compare our results to the analytical solution whenever available or to numerical results obtained using the industrial code Cast3M. In this case, we consider a linear, respectively, quadratic, cG formulation, referred to as Q1, respectively, Q2, when full integration is used, or, Q2-RI when reduced integration is used, depending on the mesh, and a three-field mixed formulation in which the unknowns are the displacement, the pressure, and the volumetric strain fields referred to as UPG; in the UPG method, the displacement field is quadratic, whereas both the pressure and the volumetric strain fields are linear. The conforming Q1 and Q2 methods with full integration, contrary to the Q2-RI method with reduced integration in most of the situations, are known to present volumetric locking due to plastic incompressibility, whereas the UPG method is known to be robust but costly. Numerical results obtained using the UPG method are used as a reference solution whenever an analytical solution is not available. A nonlinear isotropic plasticity model with a von Mises yield criterion is used for the test cases. For the first three test cases, strain-hardening plasticity is considered with the following material parameters: Young modulus $E = 206.9$ GPa, Poisson ratio $\nu = 0.29$, hardening parameter $H = 129.2$ MPa, initial yield stress $\sigma_0 = 450$ MPa, infinite yield stress $\sigma_\infty = 715$ MPa, and saturation parameter $\delta = 16.93$. For the fourth case, perfect plasticity is considered with the following material parameters: Young modulus $E = 28.85$ MPa, Poisson ratio $\nu = 0.499$, hardening parameter $H = 0$ MPa, initial and infinite yield stresses $\sigma_\infty = 6$ MPa, and saturation parameter $\delta = 0$. In the numerical experiments reported in this section, the stabilization parameter is taken to be 1, and all the quadratures use positive weights. In particular, for the HHO method, we employ a quadrature of order $Q = 2k$ for the behavior cell integration.

7.1. Plasticity small defs

Dans le cadre de la thermodynamique des milieux continus, la combinsaison de l'application des deux premiers principes de la themodynamique donne lieu à l'équation de Clausius-Duhem qui postule la positivité de l'énergie de dissipation

$$\mathcal{D} = (\underset{\sim}{\boldsymbol{\sigma}}_T - \frac{\partial \psi_\Omega}{\partial \dot{\underset{\sim}{\boldsymbol{\varepsilon}}}_T}) : \dot{\underset{\sim}{\boldsymbol{\varepsilon}}}_T - \rho \frac{\partial \psi_\Omega}{\partial v_{int}} \dot{v}_{int} \geq 0 \tag{43}$$

en l'absence de dépendence du problème à la température. Dans le cadre de l'hyper-élasticité qui est un processus de transformation réversible, comme évoque Section 2, l'ensemble V_{int} des variables internes v_{int} est supposé vide, de sorte que l'inégalité (43) revient à l'équation d'égalité (**??**). En revanche, pour des comportements dissipatifs de nature élasto-visco-plastique, on introduit un certains nombre de variables internes, qui sont liées à l'expression de l'énergie dissipée et à l'irréversibilité de la transformation. Pour des déformations infinitésimales, on suppose la décomposition additive de la déformation

$$\underset{\sim}{\boldsymbol{\varepsilon}}_T = \underset{\sim}{\boldsymbol{\varepsilon}}^e_T + \underset{\sim}{\boldsymbol{\varepsilon}}^p_T \tag{44}$$

En une partie élastique $\underset{\sim}{\boldsymbol{\varepsilon}}^e_T$ et une partie plastique $\underset{\sim}{\boldsymbol{\varepsilon}}^p_T$. En particulier, dans le cadre des matériaux standards généralisés, on suppose l'existence d'un potentiel également décomposable en une partie élastique et en une partie plastique tel que

$$\psi_\Omega = \psi^e_\Omega(\underset{\sim}{\boldsymbol{\varepsilon}}^e_T) + \psi^p_\Omega(v_{int}) \tag{45}$$

Comme évoque Section 2, le potentiel d'énergie libre de Helmoltz ψ_Ω dépend éventuellement d'un ensemble de variables internes v_{int} dans V_{int}, qui a été supposé vide jusque là. Dans le cadre d'un comportement élasto-visco-plastique, on introduit au moins une variable interne, de manière à assurer la positivité de l'énergie dissipée. Par injection de (45) dans (43), il vient que le tenseur des contraintes $\underset{\sim}{\boldsymbol{\sigma}}_T$ est la la force duale assosciées aux défromations élastiques $\underset{\sim}{\boldsymbol{\varepsilon}}^e_T$. On définit également les forces thermodynamiques V_T duales des variables internes v_{int} telles que

$$\mathcal{D} = \underset{\sim}{\boldsymbol{\sigma}}_T : \dot{\underset{\sim}{\boldsymbol{\varepsilon}}}^p_T - \rho \frac{\partial \psi_\Omega}{\partial v_{int}} \dot{v}_{int} = \begin{Bmatrix} \underset{\sim}{\boldsymbol{\sigma}}_T \\ V_T \end{Bmatrix} \cdot \begin{Bmatrix} \dot{\underset{\sim}{\boldsymbol{\varepsilon}}}^p_T \\ \dot{v}_{int} \end{Bmatrix} \geq 0 \quad \text{with} \quad V_T = -\rho \frac{\partial \psi_\Omega}{\partial v_{int}} \tag{46}$$

Par ailleurs, le cadre des matériaux standards généralisés stipule l'existence d'un convex potential ϕ containing the origin, together with a threshold function f, that define the evolution of the generalized strains such that

$$\dot{v_{int}} = \frac{\partial \phi}{\partial f} \frac{\partial f}{\partial V_T} \tag{47}$$

Le potentiel ϕ dépend de la fonction de charge f telle que celle-ci contient l'origine, est différentiable en tout point de ...

En particulier, on introduit l'ensemble des variables internes $V_{int} = \{\underset{\sim}{\boldsymbol{\varepsilon}}_T^p, p\}$ avec p la déformation plastique cumulée, et le potentiel plastique

$$\psi_\Omega^p(\underset{\sim}{\boldsymbol{\varepsilon}}_T^p, p) = \frac{K}{2}\underset{\sim}{\boldsymbol{\varepsilon}}_T^p : \underset{\sim}{\boldsymbol{\varepsilon}}_T^p + \frac{K}{2}p^2 \tag{48}$$

où K est le module d'écrouissage cinématique, et H le module d'écrouissage isotrope. Les forces thermodynamiques assosciées aux variables internes $\underset{\sim}{\boldsymbol{\varepsilon}}_T^p$ et p sont respectivement $K\underset{\sim}{\boldsymbol{\varepsilon}}_T^p$ et Hp.

$$f(\underset{\sim}{\boldsymbol{\sigma}}_T^p, q) = \sqrt{\frac{3}{2}} \tag{49}$$

We introduce the discrete logarithmic stress tensor $\underset{\sim}{\boldsymbol{E}} = 1/2\ln(\underset{\sim}{\boldsymbol{F}}_T^{\mathrm{t}} \cdot \underset{\sim}{\boldsymbol{F}}_T)$

7.2. Necking of a notched bar

In this first benchmark, we consider a 2D rectangular bar with an initial imperfection. The bar is subjected to uniaxial extension. This example has been studied previously by many authors as a necking problem 3,5,7,8,22 and can be used to test the robustness of the different methods. The bar has a length of 53.334 mm and a variable width from an initial width value of 12.826 mm at the top to a width of 12.595 mm at the center of the bar to create a geometric imperfection. A vertical displacement u y = 5mm is imposed at both ends, as shown in Figure 2A. For symmetry reasons, only one-quarter of the bar is discretized, and the mesh is composed of 400 quadrangles (see Figure 2B). The load-displacement curve is plotted in Figure 2C. We observe that, except for Q1, all the other methods give very similar results. Moreover, the equivalent plastic strain p, respectively, the trace of the Cauchy stress tensor sigma, are shown in Figure 3, respectively, in Figure 4, at the quadrature points on the final configuration. A sign of locking is the presence of strong oscillations in the trace of the Cauchy stress tensor sigma. We notice that the cG formulations Q1 and Q2 lock, contrary to the HHO, Q2-RI, and UPG methods that deliver similar results. We remark, however, that the results for HHO(1;1), HHO(1;2), and Q2-RI are slightly less smooth than for HHO(2;2), HHO(2;3), and UPG. The reason is that, on a fixed mesh, the three former methods have less quadrature points than the three latter ones (see Table 1) (HHO(2;2), HHO(2;3), and UPG have the same number of quadrature points). Therefore, the stress is evaluated using less points in HHO(1;1), HHO(1;2), and Q2-RI. It is sufficient to refine the mesh or to increase the order of the quadrature by two in HHO(1;1) and HHO(1;2) to retrieve similar results to those for the three other methods (not shown for brevity).

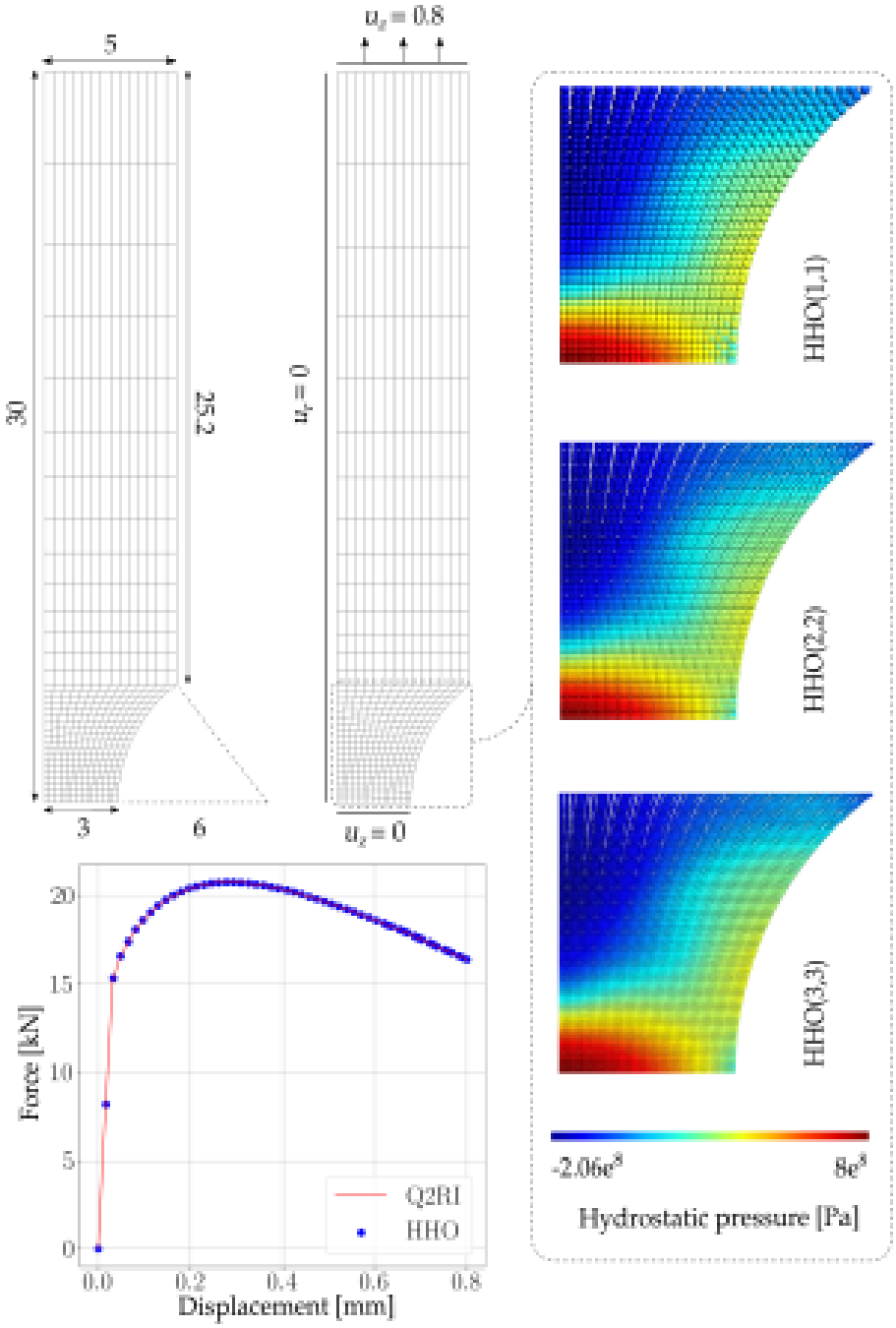

Figure 5. ssna

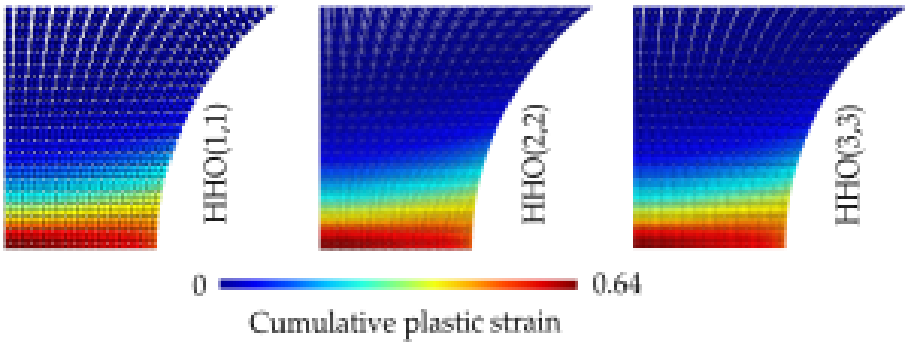

Figure 6. ssna

7.3. Quasi-incompressible sphere under internal pressure

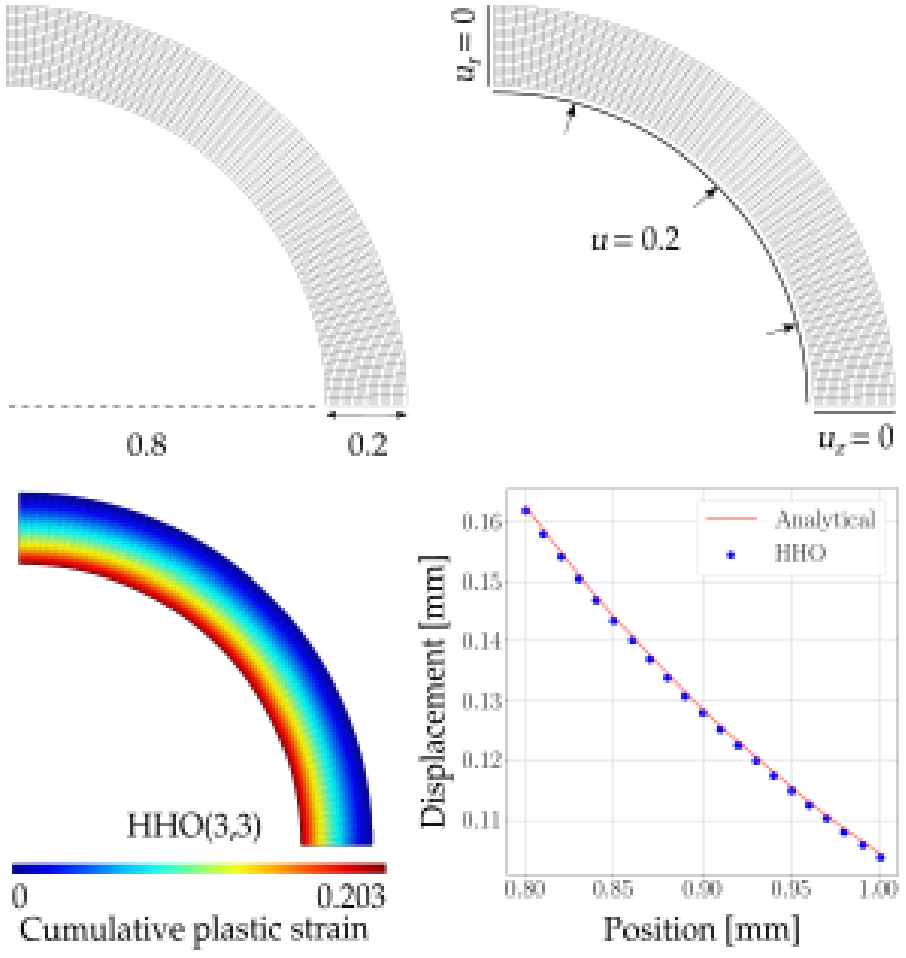

Figure 7. sphere

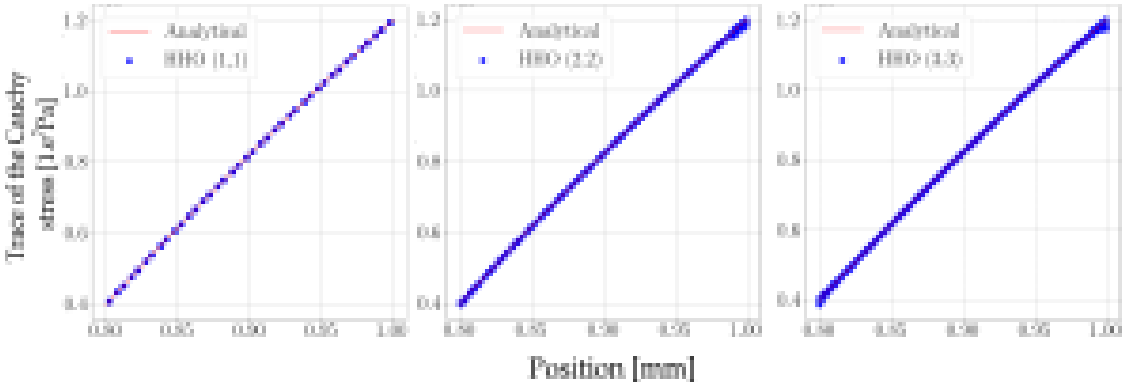

Figure 8. sphere

This last benchmark 6 consists of a quasi-incompressible sphere under internal pressure for which an analytical solution is known when the entire sphere has reached a plastic state. This benchmark is particularly challenging compared to the previous ones since we consider here perfect plasticity. The sphere has an inner radius R in = 0.8 mm and an outer radius R out = 1 mm. An internal radial pressure P is imposed. For symmetry reasons, only one-eighth of the sphere is discretized, and the mesh is composed of 1580 tetrahedra (see Figure 10A). The simulation is performed until the limit load corresponding to an internal pressure 2.54 MPa is reached. The equivalent plastic strain p is plotted for HHO(1;2) in Figure 10B, and the trace of the Cauchy stress tensor sigma is compared for HHO, UPG, and T2 methods in Figure 11 at all the quadrature points on the final configuration for the limit load. We notice that the quadratic element T2 locks, whereas HHO and UPG do not present any sign of locking and produce results that are very close to the analytical solution. However, the trace of the Cauchy stress tensor sigma is slightly more dispersed around the analytical solution for HHO(2;2) and HHO(2;3) than for HHO(1;1) and HHO(1;2) near the outer boundary. For this test case, we do not expect that HHO(2;2) and HHO(2;3) will deliver more accurate solutions than HHO(1;1) and HHO(1;2) since the geometry is discretized using tetrahedra with planar faces. We next investigate the influence of the quadrature order k Q on the accuracy of the solution. The trace of the Cauchy stress tensor sigma is compared for HHO(1;1), HHO(2;2), and UPG methods in Figure 12 at all the quadrature points on the final configuration for the limit load, and for a quadrature order k Q higher than the one employed in Figure 11 (HHO(1;2) and HHO(2;3) give similar results and are not shown for brevity). We remark that, when we increase the quadrature order, UPG locks for quasi-incompressible finite deformations, whereas HHO does not lock, and the results are (only) a bit more dispersed around the analytical solution. Moreover, HHO(2;2) is less sensitive than HHO(1;1) to the choice of the quadrature order k Q . Note that this problem is not present for HHO methods with small deformations. Furthermore, this sensitivity to the quadrature order seems to be absent for finite deformations when the elastic deformations are compressible (the plastic deformations are still incompressible). To illustrate this claim, we perform the same simulations as before but for a compressible material. The Poisson ratio is taken now as nu = 0.3 (recall that we used nu = 0.499 in the quasi-incompressible case), whereas the other material parameters are unchanged. Unfortunately, an analytical solution is no longer available in the compressible case. We compare again the trace of the Cauchy stress tensor simga for HHO(1;1), HHO(2;2), and UPG methods in Figure 13 at all the quadrature points on the final configuration and for different quadrature orders k Q . We observe a quite marginal dependence on the quadrature order for HHO methods (as in the quasi-incompressible case), whereas the UPG method still locks if the order of the quadrature is increased. Moreover, in the compressible case, HHO(2;2) gives a more accurate solution than HHO(1;1).

8. Appendix

$$\begin{aligned} J^{HW}_{I,\text{int}} :=& \int_I \psi_I + (\nabla \boldsymbol{u}_I - \underset{\sim}{\boldsymbol{G}}_I) : \underset{\sim}{\boldsymbol{P}}_I \\ =&(1-\frac{\alpha}{2}\ell)\int_{\partial K}\frac{\beta}{2h_T}\|\boldsymbol{u}_{\partial T}-\boldsymbol{u}_K|_{\partial K}\|^2 + (1-\frac{\alpha}{2}\ell)\int_{\partial K}(\boldsymbol{u}_{\partial T}-\boldsymbol{u}_K|_{\partial K})\cdot\underset{\sim}{\boldsymbol{P}}_K|_{\partial K}\cdot\boldsymbol{n} - \int_I \underset{\sim}{\boldsymbol{G}}_I : \underset{\sim}{\boldsymbol{P}}_I \end{aligned} \tag{50}$$

The development of (50) is given in Appendix. Injecting (50) in (5) yields

$$\begin{aligned} J^{HW}_T =& \int_K \psi_\Omega + (\nabla \boldsymbol{u}_K - \underset{\sim}{\boldsymbol{G}}_K) : \underset{\sim}{\boldsymbol{P}}_K + (1-\frac{\alpha}{2}\ell)\int_{\partial K}(\boldsymbol{u}_{\partial T}-\boldsymbol{u}_K|_{\partial K})\cdot\underset{\sim}{\boldsymbol{P}}_K|_{\partial K}\cdot\boldsymbol{n} \\ &+ (1-\frac{\alpha}{2}\ell)\int_{\partial K}\frac{\beta}{2h_T}\|\boldsymbol{u}_{\partial T}-\boldsymbol{u}_K|_{\partial K}\|^2 - \int_I \underset{\sim}{\boldsymbol{G}}_I : \underset{\sim}{\boldsymbol{P}}_I - \int_K \boldsymbol{f}_V\cdot\boldsymbol{u}_K - \int_I \boldsymbol{f}_V\cdot\boldsymbol{u}_I - \int_{\partial_N T}\boldsymbol{t}_{\partial_N T}\cdot\boldsymbol{u}_{\partial T} \end{aligned} \tag{51}$$

Development 8.1 (Interafce simplification). *Let $C_I = \{v \in L^2(I) \mid v\cdot\boldsymbol{n} = cste\}$ the set of L^2-functions which are constant along the normal axis in I. For any function in C_I, the following equality holds true:*

$$\int_I v\,dV = \int_{\partial K}\int_{\epsilon=0}^{\ell} v(1-\alpha\epsilon)\,dS\,d\epsilon = \ell(1-\frac{\alpha}{2}\ell)\int_{\partial K} v\,dS \tag{52}$$

Noticing that $\nabla\boldsymbol{u}_I \in C_I$, one has :

$$\begin{aligned} \int_I \psi_I =&\ell(1-\frac{\alpha}{2}\ell)\int_{\partial K}\frac{1}{2}\beta\frac{\ell}{h_T}\nabla\boldsymbol{u}_I : \nabla\boldsymbol{u}_I \\ =&\ell(1-\frac{\alpha}{2}\ell)\int_{\partial K}\frac{\beta}{2\ell h_T}(\boldsymbol{u}_{\partial T}-\boldsymbol{u}_K|_{\partial K})\otimes\boldsymbol{n} : (\boldsymbol{u}_{\partial T}-\boldsymbol{u}_K|_{\partial K})\otimes\boldsymbol{n} \\ =&\ell(1-\frac{\alpha}{2}\ell)\int_{\partial K}\frac{\beta}{2\ell h_T}\sum_{i,j}(u_{\partial T i}-u_{K i}|_{\partial K})^2 {n_j}^2 \\ =&\ell(1-\frac{\alpha}{2}\ell)\int_{\partial K}\frac{\beta}{2\ell h_T}\sum_j {n_j}^2\sum_i(u_{\partial T i}-u_{K i}|_{\partial K})^2 \\ =&\ell(1-\frac{\alpha}{2}\ell)\int_{\partial K}\frac{\beta}{2\ell h_T}\sum_i(u_{\partial T i}-u_{K i}|_{\partial K})^2 \\ =&\ell(1-\frac{\alpha}{2}\ell)\int_{\partial K}\frac{\beta}{2\ell h_T}\|\boldsymbol{u}_{\partial T}-\boldsymbol{u}_K|_{\partial K}\|^2 \\ =&(1-\frac{\alpha}{2}\ell)\int_{\partial K}\frac{\beta}{2h_T}\|\boldsymbol{u}_{\partial T}-\boldsymbol{u}_K|_{\partial K}\|^2 \end{aligned} \tag{53}$$

Moreover, for $\underset{\sim}{\boldsymbol{P}}_I$ in C_I :

$$\begin{aligned} \int_I \nabla\boldsymbol{u}_I : \underset{\sim}{\boldsymbol{P}}_I =&\ell(1-\frac{\alpha}{2}\ell)\int_{\partial K}\nabla\boldsymbol{u}_I : \underset{\sim}{\boldsymbol{P}}_I \\ =&\ell(1-\frac{\alpha}{2}\ell)\int_{\partial K}\frac{1}{\ell}(\boldsymbol{u}_{\partial T}-\boldsymbol{u}_K|_{\partial K})\otimes\boldsymbol{n} : \underset{\sim}{\boldsymbol{P}}_K|_{\partial K} \\ =&\ell(1-\frac{\alpha}{2}\ell)\int_{\partial K}\frac{1}{\ell}\sum_{i,j}(u_{\partial T i}-u_{K i}|_{\partial K})n_j P_{K ij}|_{\partial K} \\ =&\ell(1-\frac{\alpha}{2}\ell)\int_{\partial K}\frac{1}{\ell}(\boldsymbol{u}_{\partial T}-\boldsymbol{u}_K|_{\partial K})\cdot\underset{\sim}{\boldsymbol{P}}_K|_{\partial K}\cdot\boldsymbol{n} \\ =&(1-\frac{\alpha}{2}\ell)\int_{\partial K}(\boldsymbol{u}_{\partial T}-\boldsymbol{u}_K|_{\partial K})\cdot\underset{\sim}{\boldsymbol{P}}_K|_{\partial K}\cdot\boldsymbol{n} \end{aligned} \tag{54}$$

And Finally :

$$J_{I,int}^{HW} = (1 - \frac{\alpha}{2}\ell) \int_{\partial K} \frac{\beta}{2h_T} \|\boldsymbol{u}_{\partial T} - \boldsymbol{u}_K|_{\partial K}\|^2 + (1 - \frac{\alpha}{2}\ell) \int_{\partial K} (\boldsymbol{u}_{\partial T} - \boldsymbol{u}_K|_{\partial K}) \cdot \underset{\sim}{\boldsymbol{P}}_K|_{\partial K} \cdot \boldsymbol{n} - \int_I \underset{\sim}{\boldsymbol{G}}_I : \underset{\sim}{\boldsymbol{P}}_I \tag{55}$$

Development 8.2 (Elliptic projection). *Let $U^h(T) \subset U(T)$ and $U^\perp(T) \subset U(T)$ such that $U(T) = U^h(T) \oplus U^\perp(T)$, and set $\boldsymbol{u}_T = \boldsymbol{u}_T^h + \boldsymbol{u}_T^\perp$ with $\boldsymbol{u}_T^h \in U^h(T)$ and $\boldsymbol{u}_T^\perp \in U^\perp(T)$ the orthogonal projections of $\boldsymbol{u}_T$ onto $U^h(T)$ and $U^\perp(T)$ respectively. Let $V^h(\partial T) \subset V(\partial T)$ and $\boldsymbol{u}_{\partial T}^h \in V^h(\partial T)$ the orthogonal projection of $\boldsymbol{u}_T$ onto $V^h(\partial T)$. The orthogonal projection of $\boldsymbol{u}_T$ onto $U^h(\bar{T}) = U^h(T) \times V^h(\partial T)$ is then the displacement pair $(\boldsymbol{u}_T^h, \boldsymbol{u}_{\partial T}^h)$. Let $S^h(T) = \{\underset{\sim}{\boldsymbol{\tau}}_T^h \in S(T) \mid \nabla \cdot \underset{\sim}{\boldsymbol{\tau}}_T^h \in U^h(T) \mid \underset{\sim}{\boldsymbol{\tau}}_T^h|_{\partial T} \cdot \boldsymbol{n} \in V^h(\partial T)\}$, and $\underset{\sim}{\boldsymbol{G}}_T^h \in S^h(T)$ the solution of (11) for $(\boldsymbol{u}_T^h, \boldsymbol{u}_{\partial T}^h)$ such that*

$$\int_T \underset{\sim}{\boldsymbol{G}}_T^h(\boldsymbol{u}_T^h, \boldsymbol{u}_{\partial T}^h) : \underset{\sim}{\boldsymbol{\tau}}_T^h = \int_T \nabla \boldsymbol{u}_T^h : \underset{\sim}{\boldsymbol{\tau}}_T^h + \int_{\partial T} (\boldsymbol{u}_{\partial T}^h - \boldsymbol{u}_T^h|_{\partial T}) \cdot \underset{\sim}{\boldsymbol{\tau}}_T^h|_{\partial T} \cdot \boldsymbol{n} \qquad \forall \underset{\sim}{\boldsymbol{\tau}}_T^h \in S^h(T) \tag{56}$$

using the fact that $\boldsymbol{u}_{\partial T}^h$ is the projection of $\boldsymbol{u}_T$ onto $V^h(\partial T)$ and that $\underset{\sim}{\boldsymbol{\tau}}|_{\partial T} \cdot \boldsymbol{n} \in V^h(\partial T)$:

$$\begin{aligned} \int_T \underset{\sim}{\boldsymbol{G}}_T^h(\boldsymbol{u}_T^h, \boldsymbol{u}_{\partial T}^h) : \underset{\sim}{\boldsymbol{\tau}}_T^h &= \int_T \nabla \boldsymbol{u}_T^h : \underset{\sim}{\boldsymbol{\tau}}_T^h + \int_{\partial T} (\boldsymbol{u}_T|_{\partial T} - \boldsymbol{u}_T^h|_{\partial T}) \cdot \underset{\sim}{\boldsymbol{\tau}}_T^h|_{\partial T} \cdot \boldsymbol{n} \qquad && \forall \underset{\sim}{\boldsymbol{\tau}}_T^h \in S^h(T) \\ &= \int_T \nabla \boldsymbol{u}_T^h : \underset{\sim}{\boldsymbol{\tau}}_T^h + \int_{\partial T} \boldsymbol{u}_T^\perp|_{\partial T} \cdot \underset{\sim}{\boldsymbol{\tau}}_T^h|_{\partial T} \cdot \boldsymbol{n} \qquad && \forall \underset{\sim}{\boldsymbol{\tau}}_T^h \in S^h(T) \end{aligned} \tag{57}$$

using the divergence theorem and the fact that $\nabla \cdot \underset{\sim}{\boldsymbol{\tau}}_T^h \in U^h(T)$, one has :

$$\int_T \nabla \boldsymbol{u}_T^\perp : \underset{\sim}{\boldsymbol{\tau}}_T^h = \int_{\partial T} \boldsymbol{u}_T^\perp|_{\partial T} \cdot \underset{\sim}{\boldsymbol{\tau}}_T^h|_{\partial T} \cdot \boldsymbol{n} \tag{58}$$

such that :

$$\begin{aligned} \int_T \underset{\sim}{\boldsymbol{G}}_T^h(\boldsymbol{u}_T^h, \boldsymbol{u}_{\partial T}^h) : \underset{\sim}{\boldsymbol{\tau}}_T^h &= \int_T \nabla \boldsymbol{u}_T^h : \underset{\sim}{\boldsymbol{\tau}}_T^h + \int_T \nabla \boldsymbol{u}_T^\perp : \underset{\sim}{\boldsymbol{\tau}}_T^h \qquad && \forall \underset{\sim}{\boldsymbol{\tau}}_T^h \in S^h(T) \\ &= \int_T \nabla \boldsymbol{u}_T : \underset{\sim}{\boldsymbol{\tau}}_T^h \qquad && \forall \underset{\sim}{\boldsymbol{\tau}}_T^h \in S^h(T) \end{aligned} \tag{59}$$

which states that $\underset{\sim}{\boldsymbol{G}}_T^h(\boldsymbol{u}_T^h, \boldsymbol{u}_{\partial T}^h)$ is the orthogonal projection of $\nabla \boldsymbol{u}_T$ onto $S^h(T)$.

References

[1] W. Reed, T. Hill, Triangular mesh methods for the neutron transport equation, Tech. rep., United States, lA-UR–73-479 INIS Reference Number: 4080130 (1973).

[2] D. A. Di Pietro, J. Droniou, A. Ern, A Discontinuous-Skeletal Method for Advection-Diffusion-Reaction on General Meshes, SIAM Journal on Numerical Analysis 53 (5) (2015) 2135–2157. doi:10.1137/140993971.
URL http://epubs.siam.org/doi/10.1137/140993971